PERGAMON

International Journal of Multiphase Flow 26 (2000) 857–876

International Journal of Multiphase Flow

www.elsevier.com/locate/ijmulflow

Phase distribution of gas–liquid mixtures in concentric annuli-inception and termination of asymmetry

G. Das[a], P.K. Das[b,*], N.K. Purohit[a], A.K. Mitra[a]

[a]*Department of Chemical Engineering, Indian Institute of Technology, Kharagpur 721 302, India*
[b]*Department of Mechanical Engineering, Indian Institute of Technology, Kharagpur 721 302, India*

Received 29 April 1996; received in revised form 24 April 1999

Abstract

A very interesting phenomenon occurs during the simultaneous flow of gas and liquid through a vertical concentric annulus. Although the geometry is axially symmetric, the two phases distribute themselves asymmetrically over a wide range of phase velocities. The present work has attempted to investigate this asymmetric phase distribution across a cross-section through extensive experimentation by using the conductivity probe technique. The probe signals and their probability density function analysis have indicated that this feature is initiated in the bubbly-slug flow regime and persists in the entire range of slug and slug-churn flow patterns. The interfacial configuration is symmetric in bubbly, fully formed churn and the annular flow patterns. Finally, the reason for this asymmetry has been attributed to the formation of cap and Taylor bubbles which are never symmetric with respect to the axis since they always form open annular rings.

Keywords: Concentric annulus; Gas–liquid flow; Asymmetric phase distribution; Conductivity probe; PDF analysis; Cap bubble; Taylor bubble

1. Introduction

The interfacial configuration during gas–liquid two phase flow through any conduit is influenced by the flow rates and properties of the two phases, conduit geometry and the presence of any body force field. For example, stratification of the two phases occurs in inclined and horizontal tubes under the effect of gravity. However, during such flow through

* Corresponding author.

0301-9322/00/$ - see front matter
PII: S0301-9322(99)00034-8

symmetric vertical geometries, gravity does not affect the distribution of the two phases. Numerous studies (Hewitt and Hall-Taylor, 1970; Mishima and Ishii, 1984; Mc-Quillan and Whalley, 1985; Jones and Zuber, 1975, etc.) on two phase co-current upflow through circular tubes have revealed that the distribution of the two phases is symmetric with respect to the axis over a wide range of flow rates. A unique exception to this feature occurs during upflow through a concentric annulus. In this case, asymmetric phase distribution exists over a reasonably wide range of fluid velocities (Caetano et al., 1989; Kelessidis and Dukler, 1989, etc.). The present paper attempts to throw light on this typical feature of flow as well as discusses the inception and termination of asymmetry with variation in flow rates of the phases.

2. Experimental facility

The experimental facility designed for the study is shown in Fig. 1. It consists of an entry section, a vertical test section, air and water supply system and a two phase separator. The two fluids are introduced through separate openings located at diametrically opposite points. This

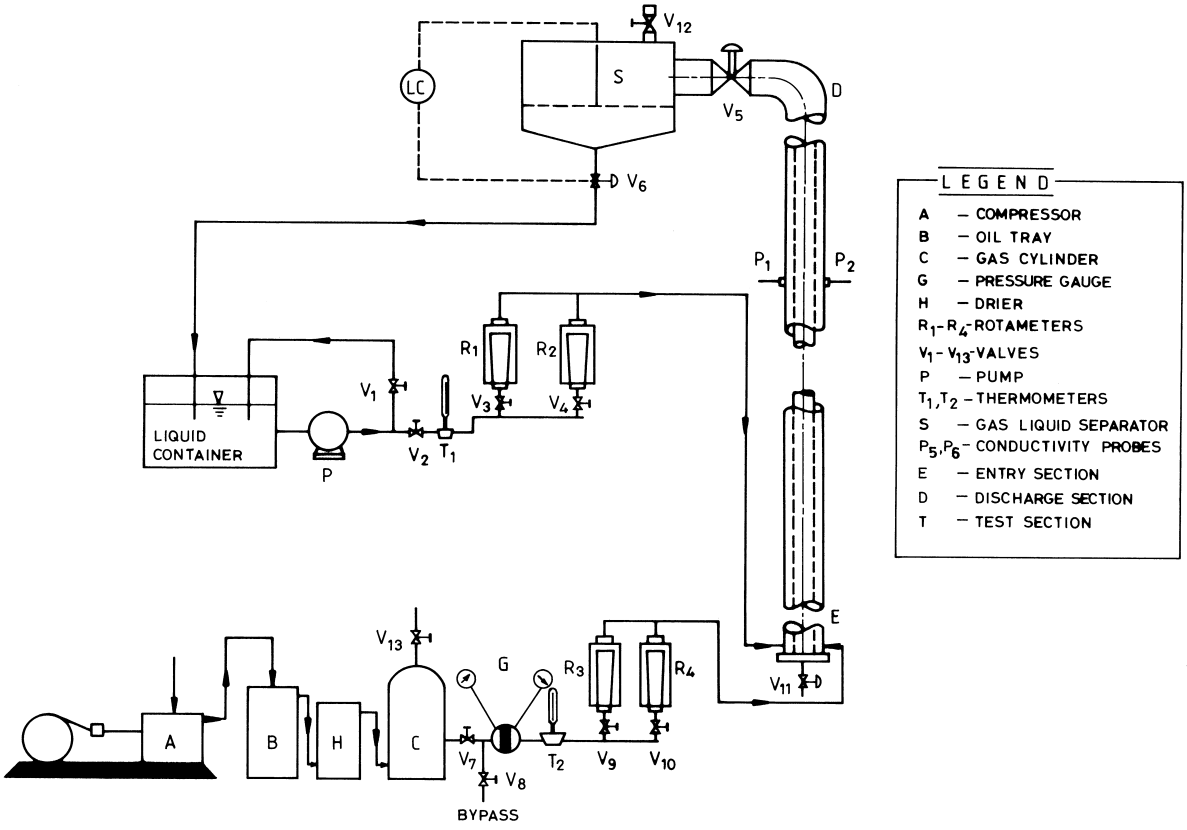

Fig. 1. Schematic diagram of the experimental set up.

section ensures that the two fluids are uniformly mixed prior to their entry into the test length. The test section is a vertical concentric annulus made of transparent outer tube to facilitate visual observation of the flow phenomenon occurring inside the passage. The inner pipe is rigidly secured at the centre of the outer pipe by a pair of specially designed flanges (F_1 and F_4) incorporated at the lower and upper end of the outer tube, as shown in the exploded view of Fig. 2. This ensures the concentricity of the test rig without producing an obstruction to the passage. Further, the concentricity has been checked during the experiments and corrective measures were taken from time to time.

An in-depth investigation of the phase distribution has been carried out using the conductivity probe technique. A unique parallel plate type conductivity probe has been indigenously designed and fabricated for this purpose. The details of the probe design and processing circuitry have been mentioned in Das (1995). A pair of probes located at diametrically opposite points in a particular cross-section have been used to note the asymmetric phase distribution at that cross-section. They have been inserted through the outer wall of the annulus at different axial positions and span the entire annular gap. The probes detect the presence of gas phase by a peak and liquid phase by a valley in the output signal. The physical appearance of the probe signals thus present a qualitative picture of the

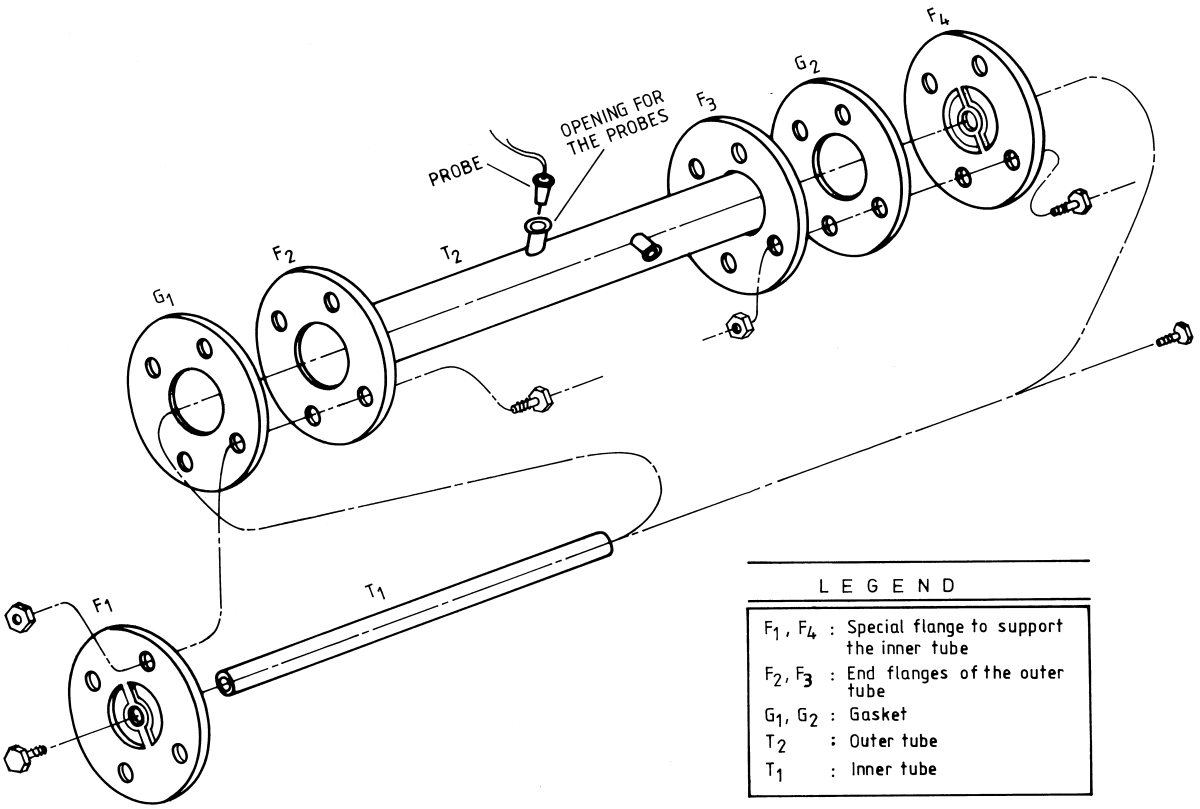

Fig. 2. Exploded view of the test section.

instantaneous phase distribution along the probe length by means of peaks and valleys recorded in the oscillographic trace. The signals have been recorded for a sufficiently long period of time for each run. This has ensured reproducible results since it eliminates the errors introduced due to the random nature of the flow.

Besides direct readout of the trace, a more quantitative measure of the signals has been used to study the phase distribution at a cross-section for the pulsating flow phenomena reported in the present paper. This is termed as the gas time ratio, t_G and is based on the times during which the continuous gas phase contacts the probe (t_a) in the total time period T of measurement. A detailed discussion of this parameter has been presented by Akagawa (1964) who has expressed t_G mathematically as

$$t_G = \frac{t_a}{T}$$

A further attempt has been made to perform the probability density function (PDF) analysis of the signals for a better appraisal of the phase distribution. Being a statistical property of the random probe signals, the PDFs presents a probabilistic nature of the phase distribution for a particular flow situation. The curves indicate the presence of the continuous water phase by a peak at zero voltage, that of air phase by a peak at maximum voltage and the presence of the dispersed phase in the continuous phase by the area under the curve between the two peaks. They are plotted with the PDF values corresponding to the voltage values as the abscissa and the ratio of voltage to maximum voltage (V/V_{max}) as the ordinate. The distribution of the two phases and their relative quantity in the flow passage is noted not only from the nature of the PDF curves but also from the ratio of the peak heights (peak ratio), the area enclosed by the peaks (area ratio) and the % area between the peaks in the curves.

Air and water have been selected as the two phases and the experiments have been carried out in three annuli with the following dimensions:

Annulus A: ID = 25.4 mm, OD = 50.8 mm;
Annulus B: ID = 12.7 mm, OD = 38.1 mm;
Annulus C: ID = 12.7 mm, OD = 25.4 mm;

The results exhibit a similar trend in the three test geometries under identical flow conditions. Moreover, the signals obtained from diametrically opposite probes at several axial locations indicate similar characteristics of phase distribution. Therefore, in order to avoid repetition, a detailed description of the results have been presented in one annulus (annulus B) for probes P_5 and P_6 only. The experiments in each annulus have been initiated at low phase velocities and the change in flow pattern has been observed by increasing the air flow rate at a particular water velocity. The figures representing the flow situation comprises of three parts. 1 depicts a pictorial description of the flow structure as observed visually. 2(a) and (b) denote the signals recorded from diametrically opposite probes P_5 and P_6, respectively, and 3(a) and (b) depict the PDF curves derived from the corresponding probe signals. In addition, some quantitative measures of the signals as well as the PDF curves for both the probes have been mentioned in a tabular form to facilitate a comparative review of the flow situation at diametrically opposite points.

3. Results and discussion

3.1. Inception of asymmetry

At low velocity of the two fluids, the flow appears to be homogeneous with discrete bubbles uniformly dispersed in the continuous water phase as is evident from Fig. 3.1. The bubbles are mostly spherical in shape and the random occurrence of a few crescent shaped bubbles does not destroy the homogeneity and symmetry of the flow situation. The similarity in the nature of the probe signals and the PDF curves obtained from diametrically opposite probes P_5 and P_6 also bears evidence to the symmetric phase distribution. Further, the close values of the gas time ratio t_G and the peak and area ratios of the PDF curves of Fig. 3 testifies the same.

On the other hand, slight asymmetry sets in the flow passage with a small increase in air flow rate. This is because the size and frequency of the cap bubbles increase and these cap bubbles are never hemispherical enclosing the inner tube completely. They are oblate spheroids and tend to rise preferentially across P_5, although this feature is not evident by visual observation and the probe signals. The PDF curves (Fig. 4.2a and b) also appear to be similar at first glance. The small differences in the quantitative measures obtained by analysing the signal recorded over a long time throws light on this.

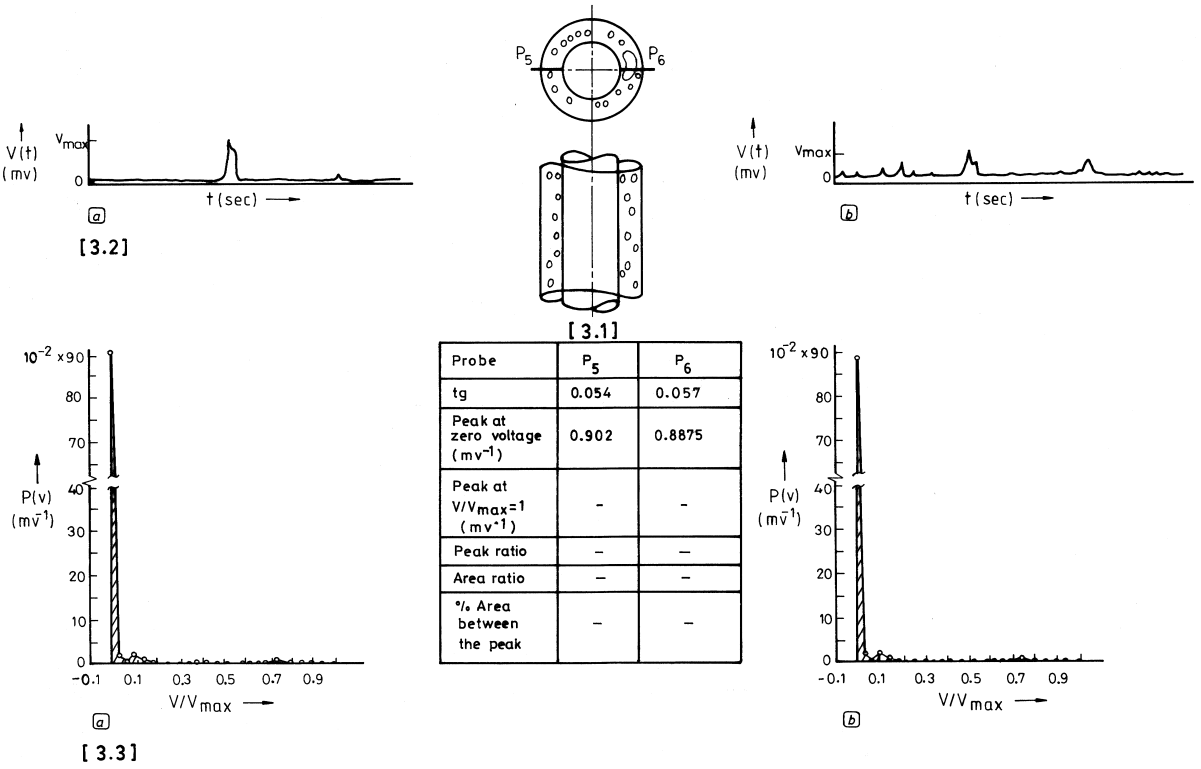

Probe	P_5	P_6
tg	0.054	0.057
Peak at zero voltage (mv^{-1})	0.902	0.8875
Peak at $V/V_{max}=1$ (mv^{-1})	–	–
Peak ratio	–	–
Area ratio	–	–
% Area between the peak	–	–

Fig. 3. Bubbly flow through Annulus B, $U_{LS} = 0.14$ m/s; $U_{GS} = 0.082$ m/s.

3.2. Growth of asymmetry

The coalescence of cap bubbles and the increase in asymmetry continues with increase of air velocity and ultimately the coalescence of the large cap bubbles result in the elongated Taylor bubbles characterising slug flow. However, the asymmetry which initiated with the inception of cap bubbles still prevails in this flow pattern. This is because the Taylor bubbles like the cap bubbles are open annular rings which do not enclose the inner tube completely. They rise along one side of the annulus and the peripheral area not occupied by the bubble is filled with a liquid bridge which extends from the inner to the outer wall of the annulus between the two edges of the bubble. An increase in air velocity primarily increases their length without changing this unique shape. A schematic view of slug flow in a circular tube and a concentric annulus has been presented in Fig. 5 to highlight the asymmetry introduced in the circular passage by a mere insertion of an inner rod in it. The figure clearly shows that, while the phase distribution in the liquid slug is symmetric in both the geometries, the configuration becomes different in the Taylor bubble region. For a better appraisal of the flow situation, the signals obtained from probes P_5 and P_6 have first been compared in Fig. 6. Both the signals appear to be similar at first sight due to the randomness of the flow situation. However, a closer examination of the two traces taken over a long period of time indicate the preference of a

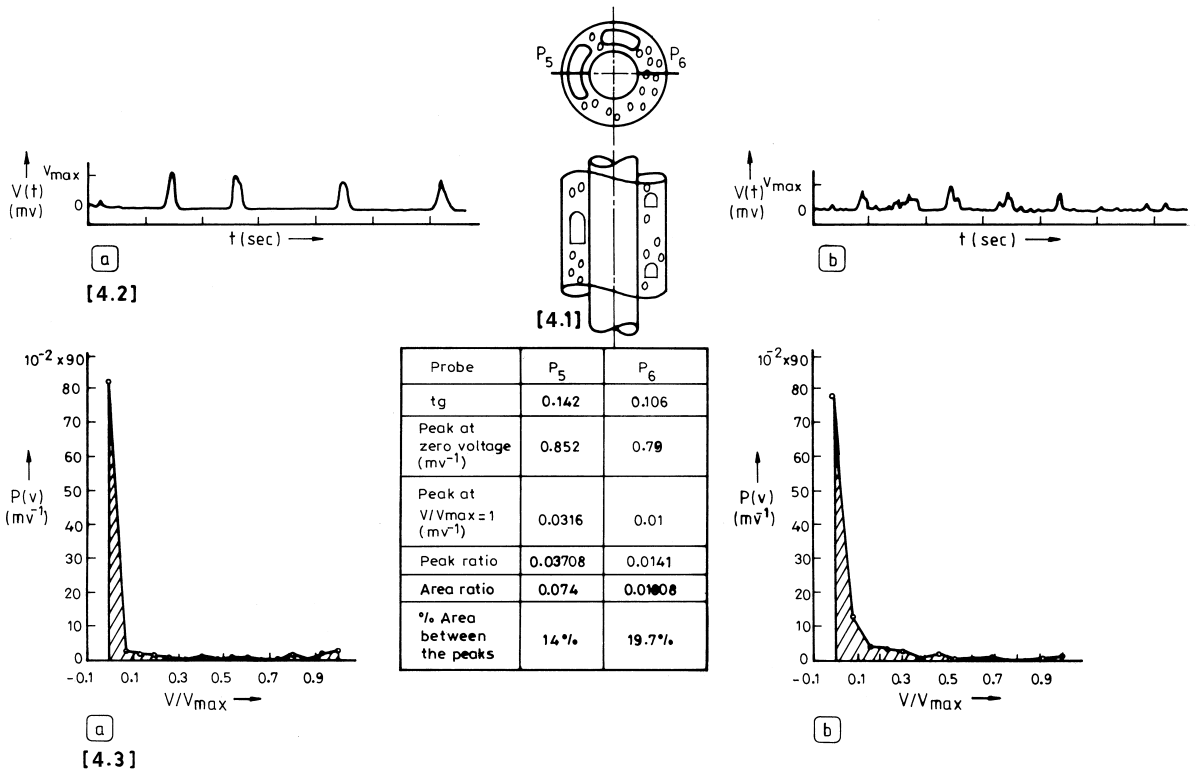

Probe	P_5	P_6
tg	0.142	0.106
Peak at zero voltage (mv^{-1})	0.852	0.79
Peak at V/Vmax = 1 (mv^{-1})	0.0316	0.01
Peak ratio	0.03708	0.0141
Area ratio	0.074	0.0108
% Area between the peaks	14%	19.7%

Fig. 4. Bubbly flow through Annulus B, $U_{LS} = 0.14$ m/s; $U_{GS} = 0.123$ m/s.

majority of the Taylor bubbles to rise along P_5 and the subtle differences in the flow structure which confirm the asymmetry of the phase distribution. It shows an increased frequency and width of the peaks and a higher value of t_G in Fig. 6.1 as compared to Fig. 6.2. One such instance has been highlighted by box B1 which is marked by a peak in (1) and a valley in (2). The figures also show the few portions where the bubbles move preferentially across P_6 (box B2) and certain areas (box B3) which are marked by peaks of almost equal width and amplitude in both the figures. These indicate the few Taylor bubbles whose orientations are such that equal length of it is traversed by both the probes. Moreover, there are a greater

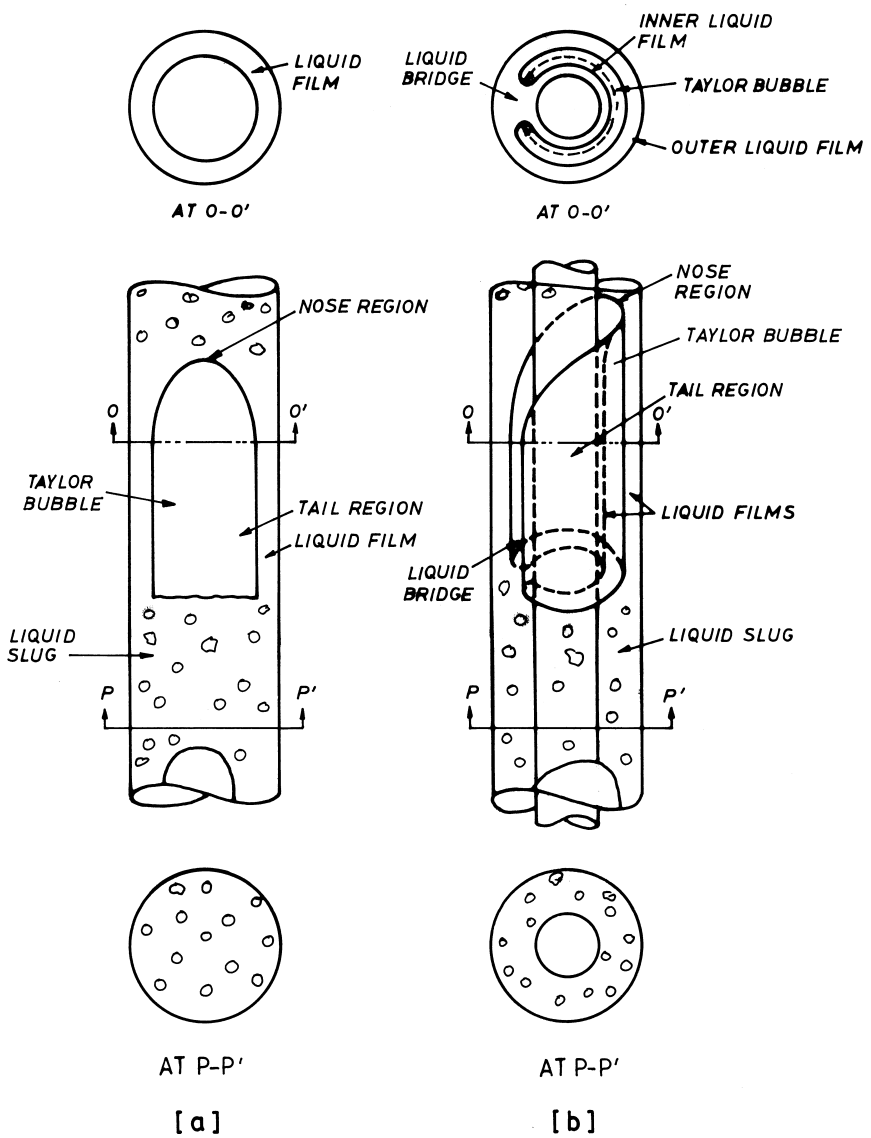

Fig. 5. Schematic representation of slug flow in (a) circular tube and (b) concentric annulus.

number of momentary pulses in Fig. 6.2 as compared to Fig. 6.1 probably due to the presence of spherical bubbles in the liquid bridge (Fig. 6) and the contact of P_6 with the edges of the bubble rising along P_5. The bimodal PDF curves of Fig. 7 also highlight the asymmetry of the flow situation in a cross-sectional plane. They confirm the preferential rise of the Taylor bubbles across P_5 by indicating a higher peak and area ratio in Fig. 7.3(a) and a higher proportion of area in Fig. 7.3(b) with a comparable zero voltage peak in two PDFs.

The asymmetry becomes more remarkable with increase in air velocity as is evident from the dissimilar nature of the probe signals depicted in Fig. 8.2 and the PDF curves of Fig. 8.3. They indicate that while the Taylor bubbles rising along P_5 become longer and slender, there is an increased bubble concentration in the liquid bridge between the edges of the Taylor bubble. The large differences in the t_G values and the ratio values are also in agreement with the visual appearance of the curves. Another unusual characteristic of the PDF curve, shown in Fig. 8.3(b), deserves special mention. The PDFs observed previously were characterised by a reduction in the zero voltage peak and a rise in the maximum voltage peak with increase of air velocity. However, in this case, the PDF exhibits a reduction in both the peaks as compared to Fig. 7.3(b) and an increase in the area between the peaks. This signifies an increased concentration of spherical bubbles in the liquid bridge with increase of air velocity leading ultimately to the breakdown of the intermittent character at P_6 and the termination of the slug flow regime.

The situation becomes more interesting at higher air velocity. Both the probe signals (Fig. 9.2) show an increase in the random oscillations in the peaks along with an increase in their width and the appearance of several triangular pulses of small width and amplitude besides the flat topped ones. This indicates that the interfacial configuration under this flow condition combine the intermittent characteristics of slug flow with the chaotic feature of churn flow. The flow, therefore, represents slug-churn transition. An inspection of the two probe signals show that while the intermittent character is still retained to some extent on the side along which a Taylor bubble prefers to rise, the flow at P_6 appears to be more chaotic. This is

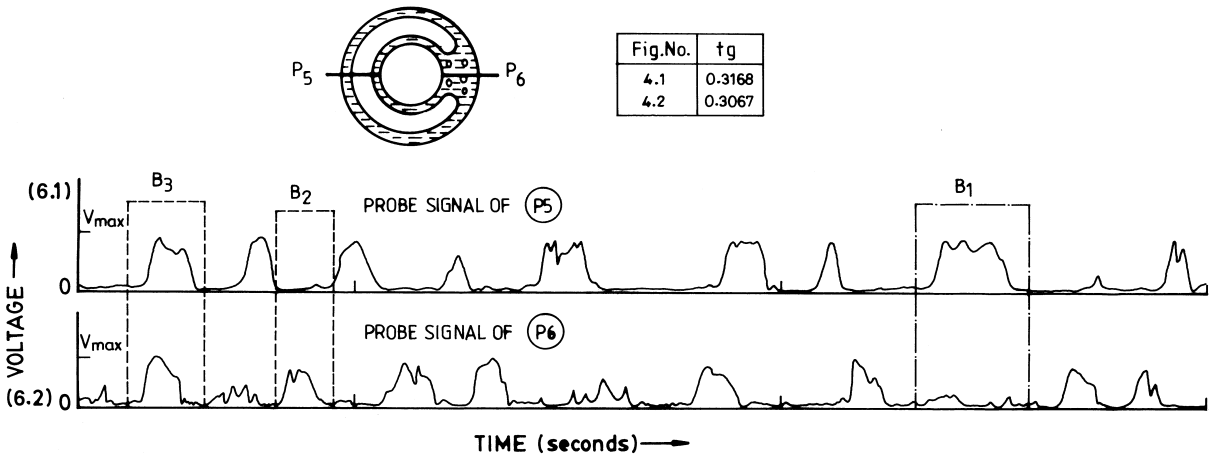

Fig. 6. Probe signals for slug flow from diametrically opposite probes in Annulus B, $U_{LS} = 0.14$ m/s; $U_{GS} = 0.344$ m/s.

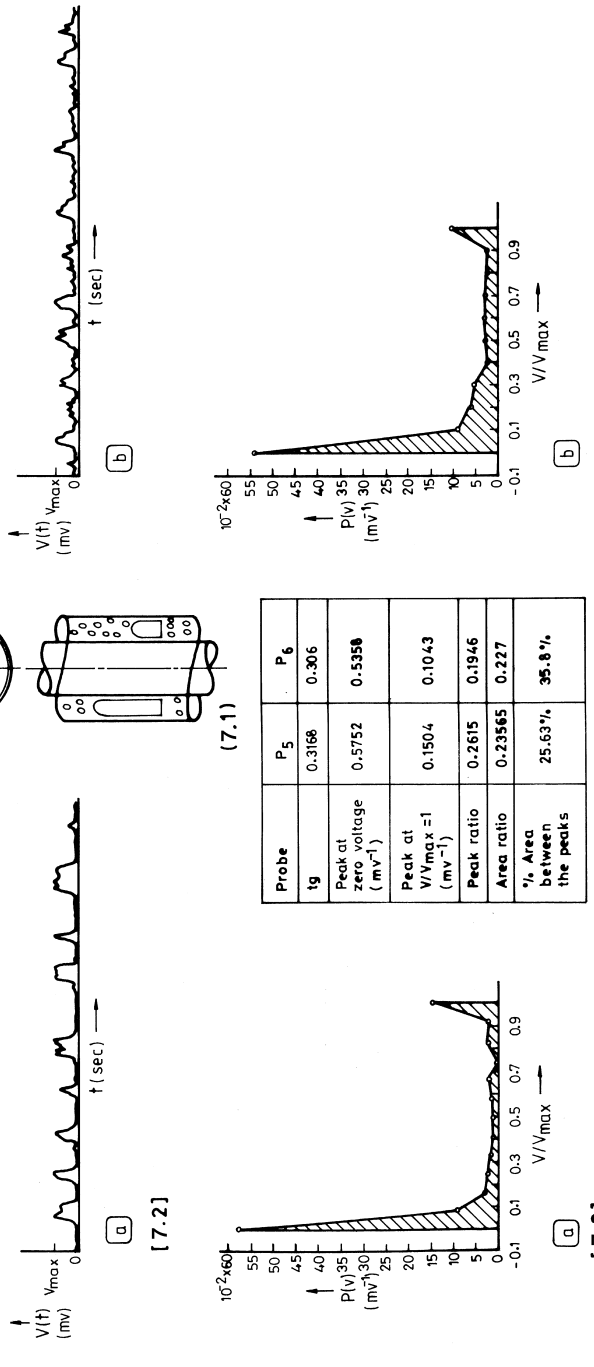

Probe	P_5	P_6
tg	0.3168	0.306
Peak at zero voltage (mv^{-1})	0.5752	0.5358
Peak at V/Vmax = 1 (mv^{-1})	0.1504	0.1043
Peak ratio	0.2615	0.1946
Area ratio	0.23565	0.227
% Area between the peaks	25.63%	35.8 %

Fig. 7. Slug flow through Annulus B, $U_{LS} = 0.14$ m/s; $U_{GS} = 0.344$ m/s.

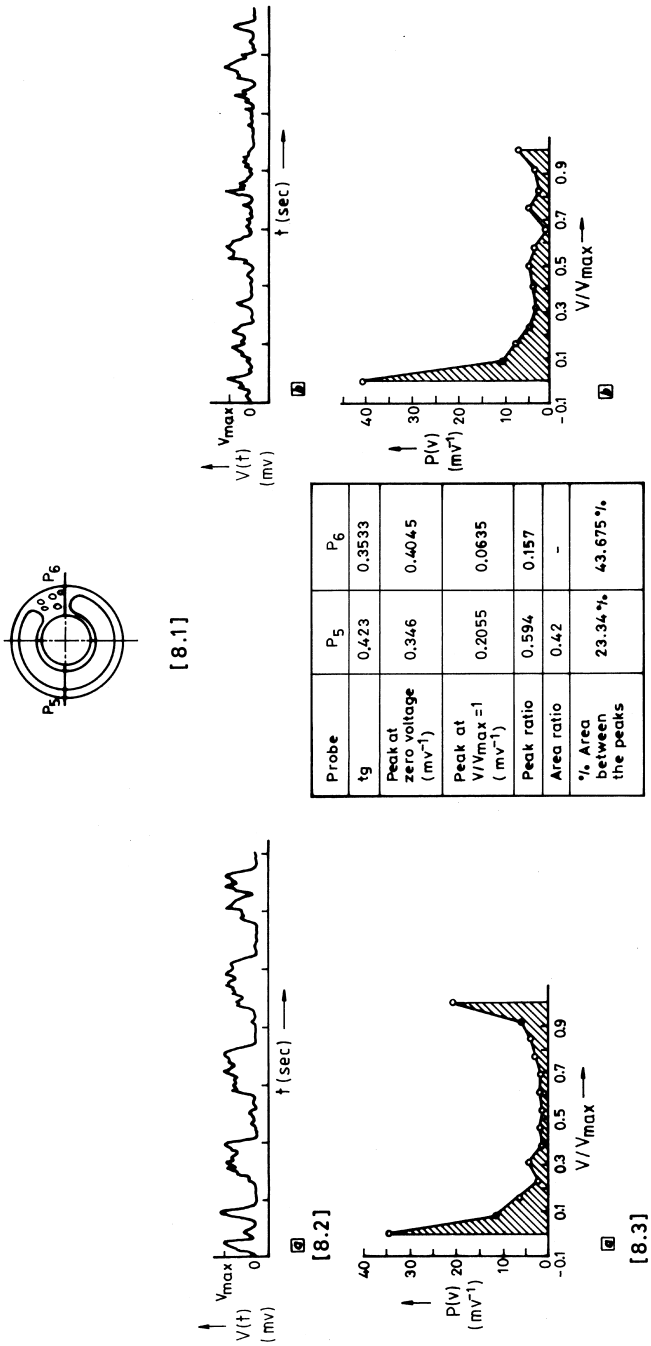

Fig. 8. Slug flow through Annulus B, $U_{LS} = 0.14$ m/s; $U_{GS} = 0.37$ m/s.

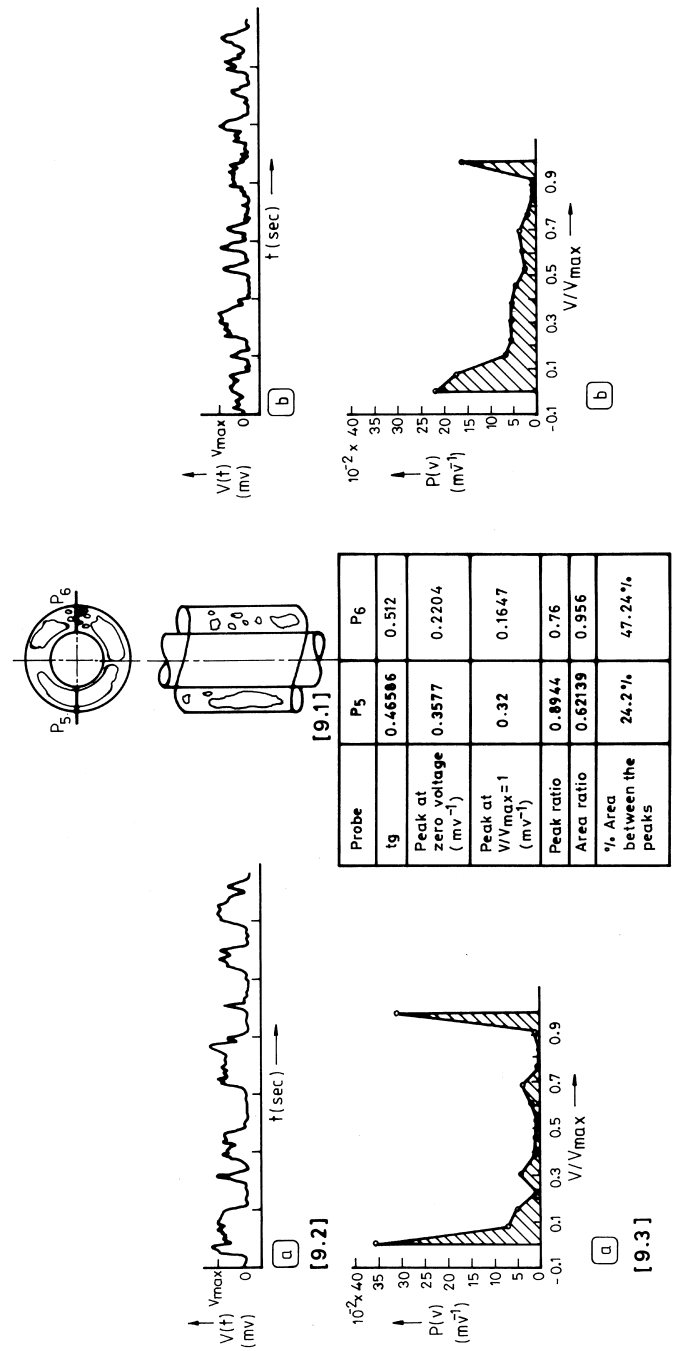

Probe	P_5	P_6
tg	0.46586	0.512
Peak at zero voltage (mv^{-1})	0.3577	0.2204
Peak at V/Vmax=1 (mv^{-1})	0.32	0.1647
Peak ratio	0.8944	0.76
Area ratio	0.6213	0.956
% Area between the peaks	24.2%	47.24%

Fig. 9. Slug flow through Annulus B, $U_{LS} = 0.14$ m/s; $U_{GS} = 0.4732$ m/s.

indicated by a large number of small width and small amplitude pulses distorting the valleys and a breakdown of the Taylor bubbles into irregular gas chunks. This once more confirms the fact that the collapse of the intermittent character of the slug flow regime is more pronounced at P_6 than at P_5. The nature of the PDF curves and the significant differences in the quantitative measures also throw light on the notable asymmetry in the cross-sectional distribution of the two phases. It may be noted that while both the peaks are distinct and large in Fig. 9.3(a), the zero voltage peak is more spread out and the % area under the curve between the two peaks is larger in Fig. 9.3(b) indicating a more random mixture of the two phases at P_6.

A further increase in air velocity makes the distribution of the two phases more chaotic with the interfacial configuration exhibiting distinct features of slug-churn transition. This is accompanied by increased differences in the interfacial structures at diametrically opposite points. Fig. 10.2(a) for probe P_5 shows pulsating probe signal between the two extreme values of voltage where the peaks and valleys are distorted by high frequency random fluctuations which are at times large enough to disrupt the steady output. Fig. 10.2(b), on the other hand, indicates random oscillations large enough to span the entire range of voltage. They tend to mask the individual peaks and valleys and the few zero voltage valleys discernible in the signal of P_5 can hardly be distinguished here. Further, the PDF curves are very different both in their appearance and quantitative measures.

3.3. Termination of asymmetry

The remarkable asymmetry in phase distribution (Fig. 10) persists over the entire range of slug-churn transition and finally terminates when the flow becomes fully developed churn with a total breakdown of the Taylor bubbles. Under such flow conditions, the signals from both the probes (Fig. 11.2(a) and (b)) show a continually oscillating and random output with the signals neither assuming 0, nor V_{max} but altogether shifting towards V_{max} indicating a higher gas voidage with increase in air velocity. Both the PDF curves of Fig. 11.3 are also similar with the absence of any peak at the extreme values of voltage and a large area under the curve from $V/V_{max} = 0$ to 1.

The probe signals and the PDF curves recorded at higher air and water velocities indicate that the phase distribution is symmetric in the entire range of the churn flow regime. As the air velocity is increased still further, the two phase mixture enters into the annular flow regime. Several signals have also been recorded from diametrically opposite probes P_5 and P_6 in the churn-annular and the annular flow regimes. All of them confirm that the symmetric phase distribution, which has been restored with the onset of the churn flow regime, remains undisturbed with further changes in flow conditions.

3.4. Effect of water velocity

The investigations when carried out at a higher water velocity indicate that water velocity shifts the onset of asymmetric phase distribution to higher air velocities since it suppresses the formation of the cap bubbles. This is evident from a comparative study of Figs. 12 and 4. Fig. 12 representing the flow situation at a higher water velocity indicates complete

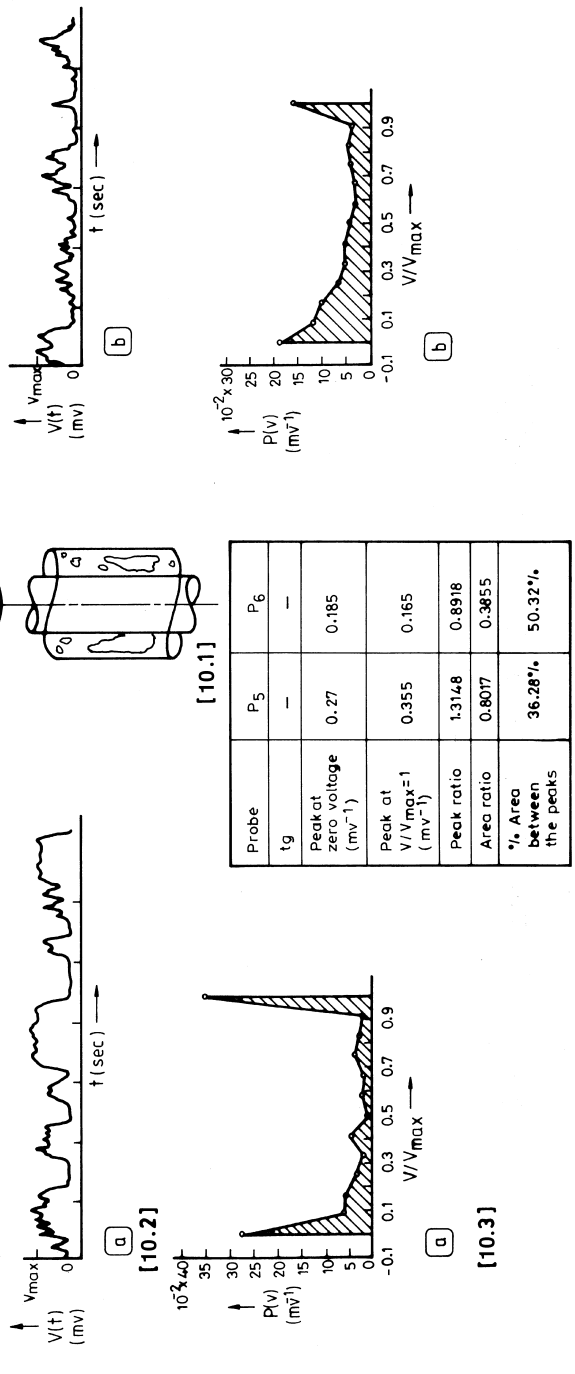

Fig. 10. Slug-churn flow through Annulus B, $U_{LS} = 0.14$ m/s; $U_{GS} = 0.6$ m/s.

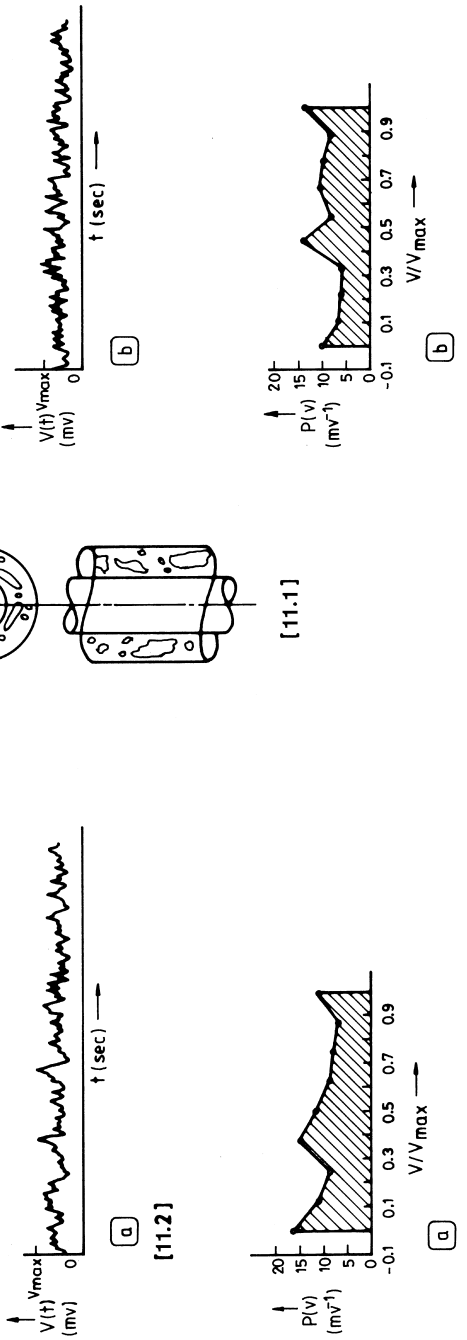

Fig. 11. Churn flow through Annulus B, $U_{LS} = 0.14$ m/s; $U_{GS} = 2.12$ m/s.

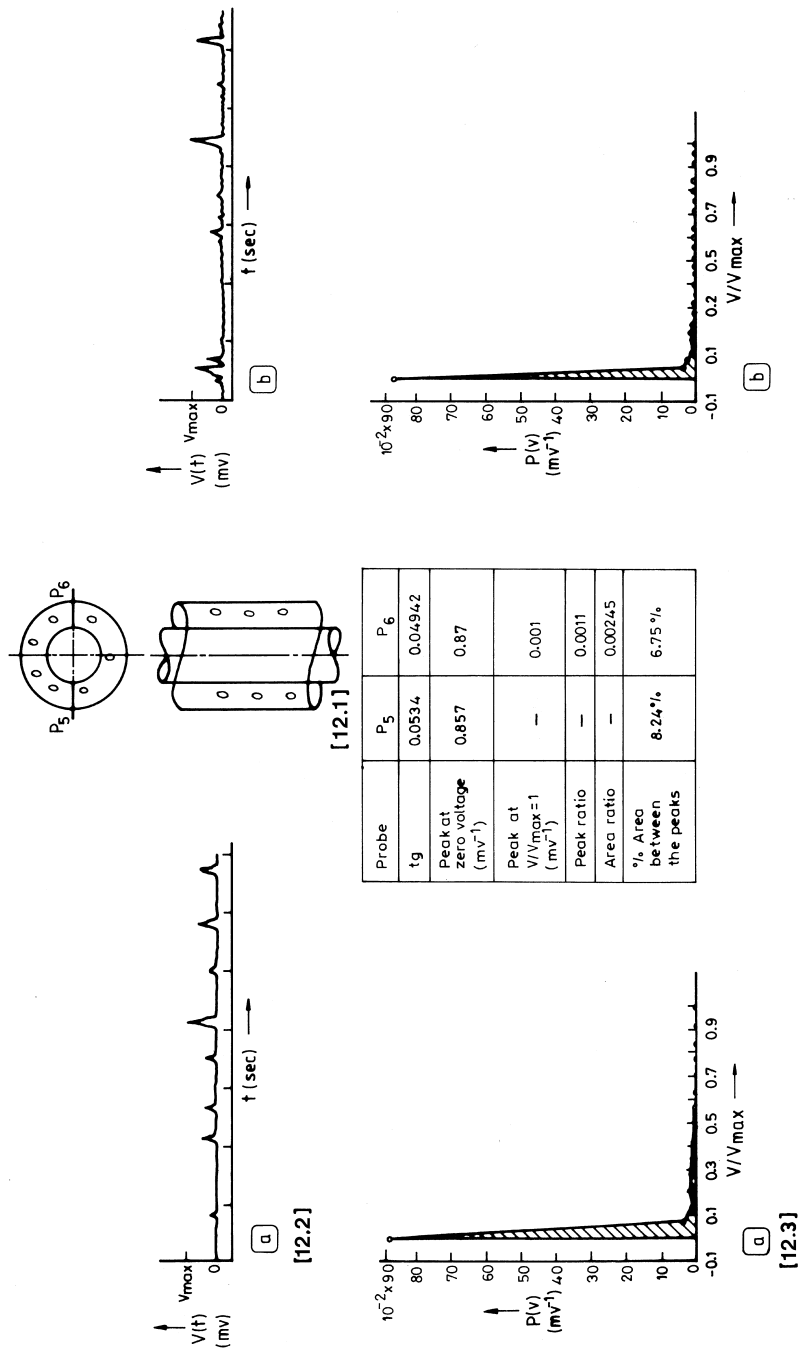

Probe	P_5	P_6
tg	0.0534	0.04942
Peak at zero voltage (mv^{-1})	0.857	0.87
Peak at V/Vmax=1 (mv^{-1})	–	0.001
Peak ratio	–	0.0011
Area ratio	–	0.00245
% Area between the peaks	8.24%	6.75 %

Fig. 12. Bubbly flow through Annulus B, $U_{LS} = 0.344$ m/s; $U_{GS} = 0.123$ m/s.

homogeneity and symmetry in the flow situation while Fig. 4 representing the flow at a lower water and same air velocity denotes an inclination towards asymmetric segregation of the two phases. However, once the cap bubbles begin to form, they coalesce to produce Taylor bubbles and the same type of phase distribution exists in the entire range of bubbly-slug, slug and the slug-churn flow regimes. Interestingly, when the water velocity is very high, both the probes record identical signals and PDF curves for the entire range of air velocities. This is because the high water velocity produces sufficient turbulent stresses to break the elongated bubbles and also suppresses further coalescence of the spherical bubbles to form cap bubbles. The flow remains dispersed bubbly for gradual increase of air velocity and it enters into the churn flow regime only at a much higher air flow rate without passing through the intermediate slug flow.

3.5. Regime of asymmetric phase distribution

A pictorial representation of the entire range of asymmetric distribution of the two phases in

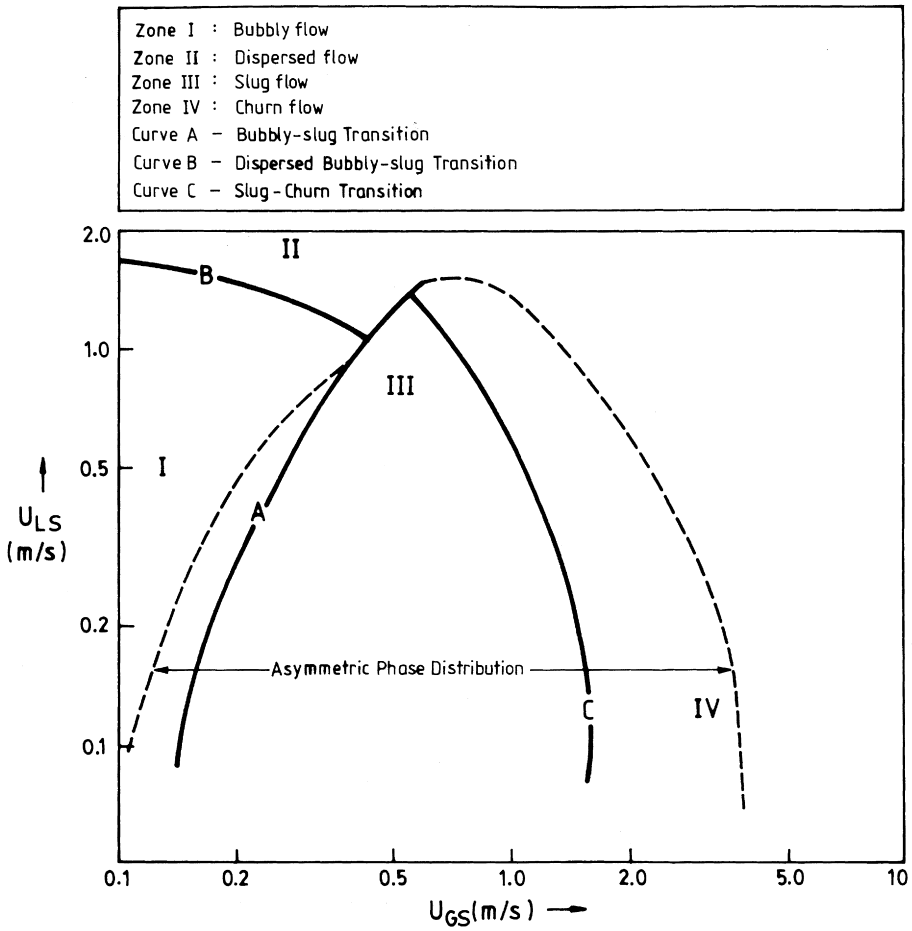

Fig. 13. Extent of asymmetric phase distribution.

terms of their superficial velocities as observed in the three annuli of the present work has been provided in Fig. 13. It denotes the inception and termination of asymmetry by means of hatched lines superimposed on the flow pattern map (Das, 1995). The gradual transition from symmetric to asymmetric and then back to symmetric phase distribution due to the gradual formation and elongation of cap bubbles and breakdown of the Taylor bubbles respectively is evident from the figure.

3.6. Effect of eccentricity on phase distribution

After noting the asymmetric phase distribution in the bubbly-slug, slug and the slug-churn flow regimes, an interest was felt to investigate the cause underlying the preferential side of rise of the cap and Taylor bubbles. An obvious cause seems to be the hydrodynamic conditions at the entry of the annular test passage which is governed by the orientation of flange F_1 (Fig. 2). The bubbles enter the test passage from the entry section through one of the free spaces of flange F_1 (shown by an arrow in Fig. 14). However, on changing the orientation of F_1 by 90°, the bubbles were observed to rise along the side perpendicular to the previous side of rise. This arises due to the fact that the bubble always prefer to rise along the path of least resistance. While the entry conditions determine the plane of bubble rise, it has been felt that the choice between the two free spaces in the flange F_1 might be governed by the small eccentricity of the annulus in one plane. Although the specially designed flanges ensure the concentricity at the entry and exit positions, a deviation in the concentricity at any intermediate circumferential plane despite the best of our efforts can not be ruled out. In order to note the effect of eccentricity on the preferential side of bubble rise, an elaborate experimentation has been planned.

For this, we had constructed two annular test sections (Fig. 15) with inside and outside diameters identical to that of annulus B. In test section D, a straight inner tube has been inserted in the outer cylinder so that the plane of eccentricity is fixed throughout the test length. On the other hand, in test section E, the inner cylinder is made of two straight tubes of equal diameter connected end to end vertically with a small axial offset, where the centre to

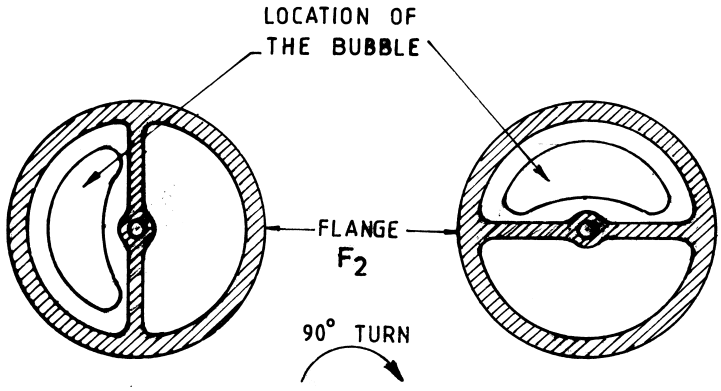

Fig. 14. Preferential side of bubble rise at different orientation of the split flange.

centre distance between the outer and the inner cylinders has been kept constant at 9.5 mm. Thus, the eccentricity in annulus E although constant, changes from one side to another side of the test section at the midplane. The experiments in annulus D have been conducted both for a fully eccentric (inner cylinder touching the outer cylinder) annulus and for an annulus with an eccentricity value of 0.5. The experiments have been performed both by introducing measured volumes of air in water filled annular columns as well as during the simultaneous flow of the two fluids.

The Taylor bubbles in both annuli D and E, were observed to rise along the wider gap during slug flow as well as in stationary water columns. Interestingly in annulus E, they are seen to change their side of rise abruptly at the mid-plane of the test section where the eccentricity has been changed from one angular plane to another. This is in contrary to the results in our concentric set up where the Taylor bubbles have always risen along one side of the test passage and not changed side during their upward propagation. This shows that there is no appreciable change in eccentricity from one circumferential plane to another in our test

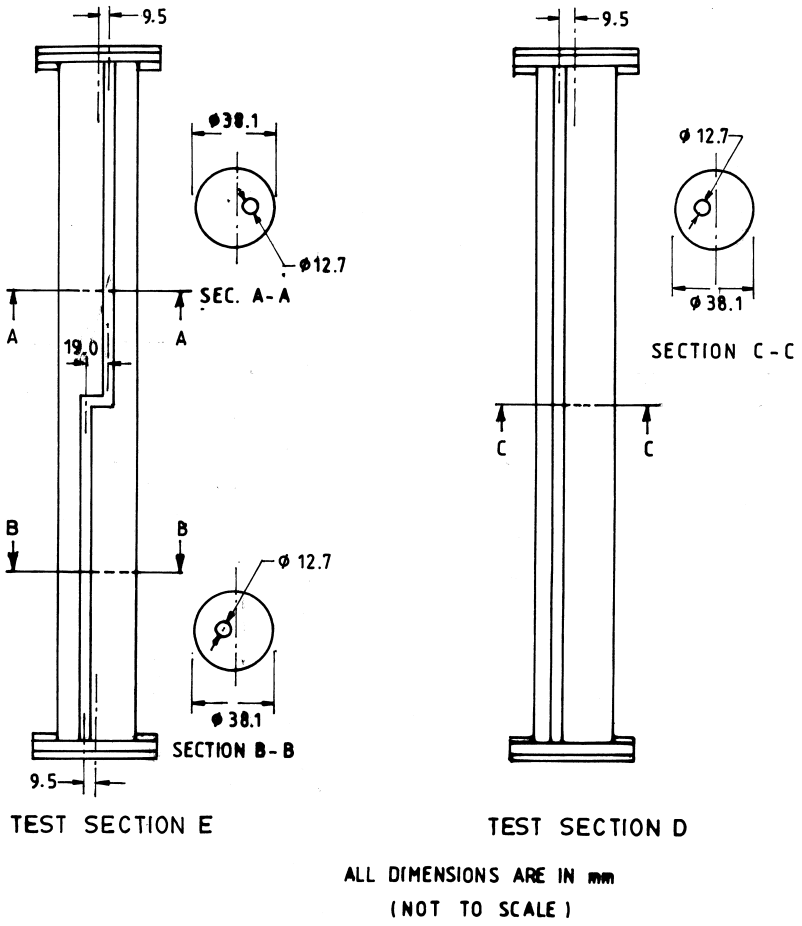

Fig. 15. Schematic diagrams of the test sections D and E.

rig (Fig. 1). The eccentricity which might have existed due to the incorporation of the special flanges is also negligible and incidentally on the same side. This has been further verified by measurements of rise velocities of these bubbles in stationary water columns. The results indicate that all the rise velocity data in the eccentric annuli are less than that obtained in the concentric set up (Das, 1995). Thus, the preferential side of rise of the Taylor bubbles along one side of the annulus occurs primarily due to the hydrodynamic conditions at the entry and probably due to a small eccentricity within experimental limits that exist in the test sections.

4. Conclusion

It is obvious from the above discussions that the insertion of a rod in a circular tube introduces remarkable asymmetry in the distribution of the two phases over a considerable range of their flow rates. This further complicates the complex behaviour of gas–liquid two phase upflow and needs to be incorporated in any model required to predict the hydrodynamics of such flow in an annulus. The reason behind the asymmetry is the formation of the asymmetric cap and Taylor bubbles which are characterised by their typical shape resulting in dissimilar phase distribution across a particular cross-section in the bubble-slug, slug and slug-churn flow regimes. Kelessidis and Dukler (1990) have also observed such Taylor bubbles in water filled vertical annulus. They have shown that these bubbles in an annulus have to be asymmetric in order to rise at the maximum possible velocity. However, the bubbly as well as the churn flow regime is symmetric at a diametral plane due to the absence of the cap and Taylor bubbles. On the other hand, the distribution of the two phases remain uniform across a particular cross-section at high mixture velocities. The high velocity of the two phases produce sufficient turbulence to breakdown the Taylor bubbles and prevent further recoalescence of the smaller ones. This results in dispersed bubbly flow at low air velocity which subsequently shifts to churn flow without the intermediate slug flow regime.

Acknowledgements

We acknowledge the reviewers and the editor for their valuable suggestions.

References

Akagawa, K., 1964. Fluctuations of void ratio in two phase flow, first report, the properties in a vertical upward flow. Bull. of JSME 7 (25), 122–128.

Caetano, F.F., Shoham, O., Brill, J.P., 1989. Upward vertical two phase flow through annulus. Part I: Single phase friction factor, taylor bubble rise velocity and flow pattern prediction, multiphase flow. In: Proc. 4th Int. Conf. BHRA, Cranfield, England, 301–330.

Das, G., 1995. Some hydrodynamic aspects of two phase gas–liquid upflow through concentric annulus, Ph.D. thesis, IIT Kharagpur, India.

Hewitt, G.F., Hall-Taylor, N.S., 1995. Annular Two Phase Flow. Pergamon Press, New York.

Jones, O.C., Zuber, N., 1975. The interrelation between void fraction fluctuations and flow patterns in two phase flow. Int. J. Multiphase Flow 2, 273–306.

Kelessidis, V.C., Dukler, A.E., 1989. Modelling flow pattern transitions for upward gas–liquid flow in vertical concentric and eccentric annuli. Int. J. Multiphase Flow 15, 173–191.

Kelessidis, V.C., Dukler, A.E., 1990. Motion of large gas bubbles through liquids in vertical concentric and eccentric annuli. Int. J. Multiphase Flow 16 (3), 375–390.

Mc-Quillan, K.W., Whalley, P.B., 1985. Flow pattern in vertical two phase flow. Int. J. Multiphase Flow 11, 161–175.

Mishima, K., Ishii, I., 1984. Flow regime transition criteria for two phase flow in vertical tubes. Int. J. Heat Mass Transfer 27, 723–734.